^{13}C CPMAS NMR spectroscopy as a probe for porphyrin–porphyrin and host–guest interactions in the solid state

Nick Bampos,[a] Michèle R. Prinsep,[b] Heyong He,[a] Anton Vidal-Ferran,[a] Alan Bashall,[c] Mary McPartlin,[c] Harry Powell[d] and Jeremy K. M. Sanders*,†[a]

[a] *Centre for Molecular Recognition, University Chemical Laboratory, Lensfield Road, Cambridge, UK CB2 1EW*
[b] *Department of Chemistry, University of Waikato, Private Bag 3105, Hamilton, New Zealand*
[c] *School of Chemistry, University of North London, Holloway Road, London, UK N7 8DB*
[d] *Cambridge Crystallographic Data Centre, 12 Union Road, Cambridge, UK CB2 1EZ*

Solid-state ^{13}C cross-polarisation magic-angle spinning (CPMAS) NMR spectra of a range of metallo-porphyrin monomers, dimers, trimers and various host–guest adducts have been obtained. Interpretation of these spectra provides information on crystal packing (molecular stacking) and host–guest interactions in the solid state. X-Ray structures are reported for a *para*- and *meta*-substituted zinc porphyrin monomer. Comparison of the CPMAS data with the X-ray data of these selected monomers provides convincing evidence for the crystal packing assignment based on both solid state techniques.

In any investigation of molecular structure, it is essential to establish a pattern for a class of compounds using various spectroscopic techniques. Single crystal X-ray diffraction analysis provides the greatest detail and in most cases, would only need a small number of crystal structures to define a class, or to investigate a limited number of compounds that may possess unique properties within a class. Most often, porphyrins are obtained as fine powders and single crystals suitable for X-ray diffraction analysis are difficult to obtain, the method of crystallisation being by no means predictable. It would be generally useful to employ NMR spectroscopy to screen families of structures that have been characterised by X-ray analysis of a limited number of molecules or complexes within a class.

The development in nuclear magnetic resonance (NMR) spectroscopy of the cross-polarisation, magic-angle spinning (CPMAS) experiment,[1,2] offers chemists a powerful tool with which to analyse a vast array of compounds in the solid state.[3] In contrast to the properties of molecules in the solution state (the study of which is well established using high resolution NMR spectroscopy[4]), the solid state can yield valuable additional information concerning intermolecular interactions and chemical exchange. Porphyrins and their analogues constitute an important class of molecules which are prevalent in nature and facilitate an extensive series of chemical reactions.[5] In the free-base (metal-free) form, porphyrins exhibit tautomerism characterised by migration of the inner hydrogens between pairs of nitrogen atoms. This exchange has been studied in the solution state,[6] although the mechanism was not clearly understood. A series of elegant ^{13}C and ^{15}N CPMAS NMR experiments[7–11] have contributed to the understanding of the mechanism, and suggest that the rate of exchange (in the solid state) is dependent on the crystal packing for a series of porphyrins.[9] These studies were significant in helping clarify the anomalous interpretation of the tautomerism derived from X-ray analysis[10] and confirm CPMAS NMR as a useful spectroscopic tool in porphyrin chemical analysis.

Porphyrin 'host' compounds are difficult to crystallise and when suitable crystals are obtained, the ensuing X-ray diffraction studies are not straightforward.[12,13] Typically, large ring currents and intermolecular offsets due to π–π repulsion cause sizeable shifts in the solid state spectra of porphyrin compounds.[14,15] Symmetry breaking effects in the solid state (in contrast to the isotropic motion of the molecules in the solution state) have already been observed in the ^{13}C CPMAS NMR spectra of *meso*-porphyrins.[4a] In this work, we present the results of a systematic investigation of a series of symmetrical (C_2) porphyrin compounds (**1**–**12**) and host–guest complexes (**13**–**18**; **8**–**18** were constructed from **2** as the basic building block) by ^{13}C CPMAS NMR spectroscopy and find, as

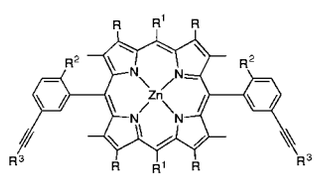

R = CH_2CH_2COOMe

1 R^1 = H, R^2 = H, R^3 = $SiMe_3$
2 R^1 = H, R^2 = H, R^3 = H
3 R^1 = H, R^2 = I, R^3 = I
4 R^1 = H, R^2 = OMe, R^3 = $SiMe_3$
5 R^1 = NO_2, R^2 = H, R^3 = $SiMe_3$

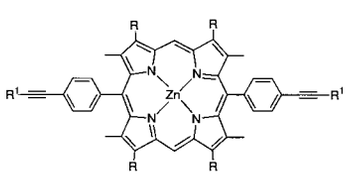

R = CH_2CH_2COOMe

6 R^1 = $SiMe_3$
7 R^1 = H

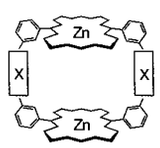

8 X = $CH_2CH_2CH_2CH_2$
9 X = C≡C
10 X = C≡C–C≡C

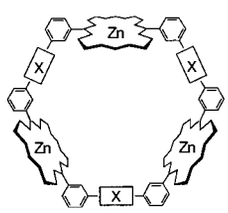

11 X = C≡C–C≡C
12 X = $CH_2CH_2CH_2CH_2$

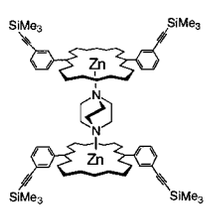

13

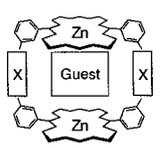

14 X = C≡C, Guest = DABCO
15 X = $CH_2CH_2CH_2CH_2$, Guest = DABCO
16 X = C≡C–C≡C, Guest = BiPy

† E-Mail: jkms@cam.ac.uk

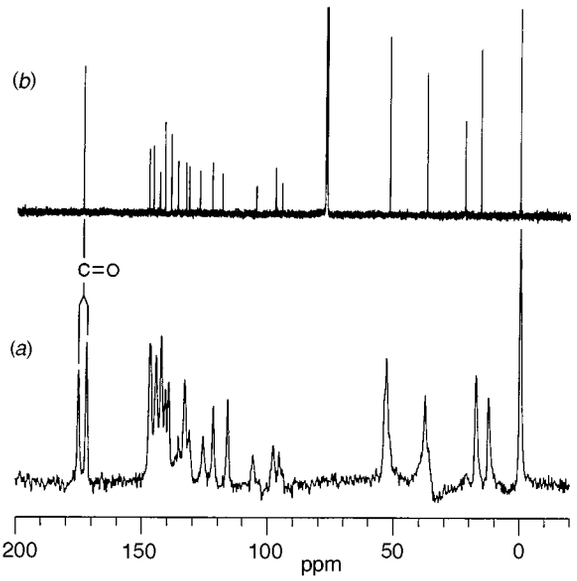

Fig. 1 (*a*) ^{13}C CPMAS NMR (100.6 MHz) spectrum and (*b*) solution ^{13}C NMR spectrum (100.6 MHz, $CDCl_3$) of the Zn *meta*-substituted monomer **1**; assignment of resonances is presented in the Experimental section

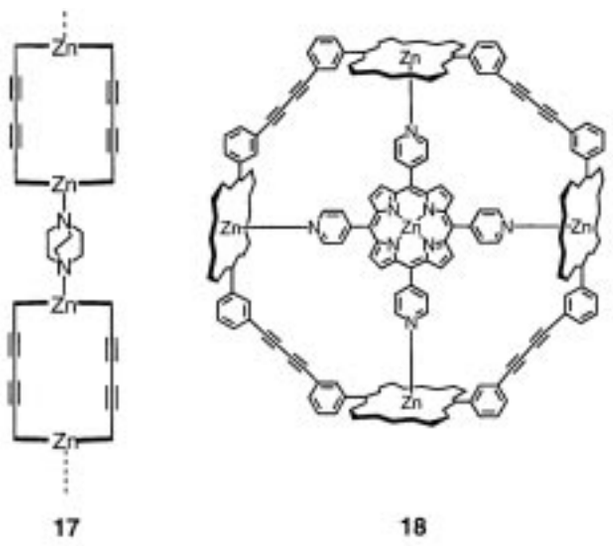

expected, that symmetry breaking effects are indeed generally observed, except where electronic or steric contributions, or the combination of host and ligand interactions enforce vertical (non-offset) stacking. Our conclusions are strengthened by two key X-ray structures.

Results and discussion

Porphyrin monomers

Fig. 1(*a*) shows the ^{13}C CPMAS NMR spectrum of *meta* substituted-ditrimethylsilyl (TMS) zinc monomer **1**, while Fig. 1(*b*) shows the solution state spectrum of the same molecule, for comparison. The linewidths of solid state NMR spectra are typically broader than those seen in the solution state and in the best solid state spectra we obtained, linewidths were recorded in the order of 1 ppm, which compares favourably with previous reports.[4a]

Various properties of molecules in solution average out effects that would otherwise lead to line broadening,[2,16] but such averaging is not possible for solids on account of their 'static' nature. Solid state spectra of monomers (with ester side-chains) (**1**–**7**) were assigned, where possible, by comparison with the corresponding solution state spectra recorded in $CDCl_3$ or

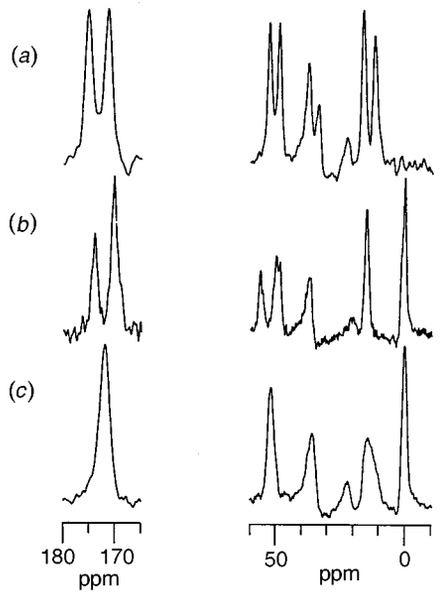

Fig. 2 Carbonyl (low field) and aliphatic (high field) regions of the ^{13}C CPMAS NMR (100.6 MHz) spectrum of (*a*) Zn *meta*-substituted monomer **2**, (*b*) Zn *meta*-substituted (methoxy) monomer **4** and (*c*) Zn *meta*-substituted (dinitro) monomer **5**

C_5D_5N. The high field region of the spectra from 0–60 ppm (methyl and methylene signals), the mid-field region from 60–120 ppm (*meso* and acetylenic signals) and the low field region from 150–180 ppm (aromatic and carbonyl signals) were all diagnostic and could be easily assigned, while resonance in the congested region between 120–150 ppm were broad (due to overlap) and difficult to assign.

A characteristic feature of the ^{13}C CPMAS NMR spectra for the majority of metalloporphyrin monomers investigated, was the presence of (at least) two carbonyl signals between 150–180 ppm (Figs. 1 and 2). The separation between these signals ranged from 3.2 ppm for the TMS protected free-base form of monomer **1** to 3.9 ppm for the deprotected zinc monomer **2**. Split signals were also evident in the high field region of the spectra of some of the monomers. For example, in the solid state spectrum of the de-protected zinc monomer **2**, the methoxy carbon, both methylene signals of the ester side-chain and the pyrrole ring methyl signal were all clearly split [Fig. 2(*a*)].

The splitting of signals in the ^{13}C CPMAS NMR spectra of the metalloporphyrin monomers examined in this work may reflect the presence of more than one solid phase, the nature of the asymmetric unit (*i.e.* if the asymmetric unit defines the whole molecule or part of it) or the off-centre stacking[17] of the individual molecules. It follows from the final point that the off-centre arrangement (horizontal displacement) is a result of the repulsive interaction of the π-electron systems and acts to minimise π–π interaction.[15] This stacking arrangement is such that some groups on one porphyrin molecule will either lie in the shielding or deshielding regions of the ring current generated by a neighbouring porphyrin molecule, resulting in the splitting of the appropriate signals in the ^{13}C CPMAS NMR spectrum. For the series of monomers examined, it is the methyl ester side-chains and pyrrole ring methyl groups (in effect half the molecule) that would lie across a porphyrin ring, above or beneath it in any resulting stack and therefore be most affected by the ring current. In the absence of X-ray data for the *meta*-substituted aryl monomers, we might predict that half the molecule defines the asymmetric unit. If this were the case we would expect two sets of signals, and the spectra of most of the monomers corroborate this, with carbonyl signals generally split, in addition to the resonances of the ring methyl groups and other carbons of the ester side-chains, while some of the other antici-

pated signals may be absorbed in the line broadening of neighbouring peaks.

The only ^{13}C CPMAS NMR spectrum of a monomer to show no splitting of the carbonyl signal was that of the dinitro-TMS protected monomer **5** [Fig. 2(*c*)]. In the absence of crystallographic evidence, one can imagine several reasons for this. The dinitroporphyrin exhibits a marginally reduced ring current with which to influence chemical shifts, but this effect is probably not significant.[18] More importantly, removal of electron density from the ring system by the strongly electron withdrawing nitro groups will diminish the π–π repulsive interaction between molecules and as a consequence allow the molecules to stack 'vertically' instead of offset.[15] This effect will eliminate the differential shielding of the ester side-chains by the ring current of adjacent porphyrins. It is worth noting, however, that the dinitro monomer is the only example of a dodeca-substituted metalloporphyrin investigated in this work. Evidence from X-ray crystal structures of various dodeca-substituted porphyrins suggests that the shape of these molecules depends on the nature of the *meso* substituents.[19] If the *meso* substituents are sp^3 hybridised, then the porphyrin will assume a 'ruffled' conformation. If the substituents are sp^2 hybridised (*e.g.* nitro groups), the porphyrin molecule will assume a saddle conformation, with each pyrrole ring in the structure displaced alternately above and below the molecular plane. It therefore follows that the dodeca-substituted dinitro monomer might also assume a distorted (saddle) shape in the crystal, or at the very least be substantially non-planar. Comparison with other dodeca-substituted examples in the literature suggests that in the solid state, crystallisation would give vertical stacks rather than a horizontal displacement of molecules.[20] The observed ^{13}C CPMAS spectrum of the dinitro monomer is consistent with this proposition.

The ^{13}C CPMAS NMR spectrum of the *para*-substituted TMS protected zinc monomer **6** [Fig. 3(*a*)] differs from the spectra shown in Figs. 1 and 2, in that it appears that every signal in the spectrum is split, including the trimethylsilyl signal. In addition to this, the carbonyl signal is split into four peaks, although the two central ones are not well resolved.

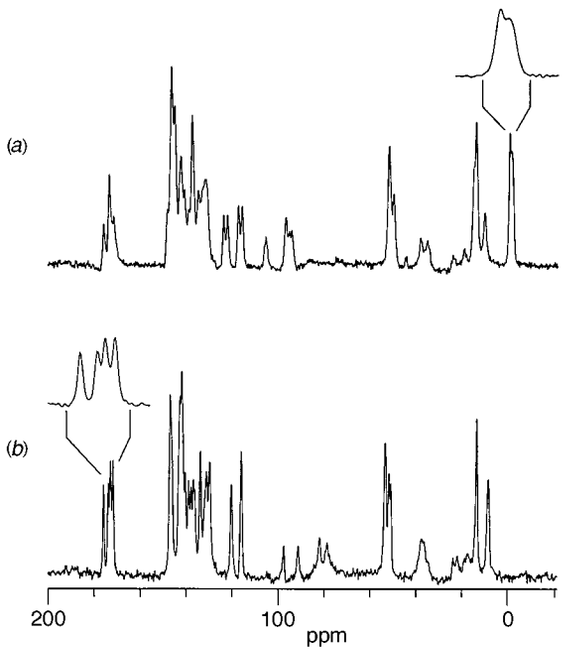

Fig. 3 ^{13}C CPMAS NMR (100.6 MHz) spectrum of (*a*) Zn *para*-substituted monomer **6**, with expansion of the TMS resonances around 0 ppm, and (*b*) Zn *para*-substituted monomer **7**, with expansion of the low field carbonyl resonances around 173 ppm

From the point of view of the porphyrin ring, this molecule has the same symmetry as the other monomers, yet the ^{13}C CPMAS NMR spectrum indicates that the change in the aryl substitution pattern dramatically affects the packing in the solid state. In order to observe four different carbonyl signals in the spectrum, all four carbonyl groups in one molecule must be inequivalent or the entire molecule must consistute the asymmetric unit. From the X-ray structure (Fig. 4) it is possible to see that the whole molecule forms the asymmetric unit (see latter) and that in terms of π-stacking two molecules are

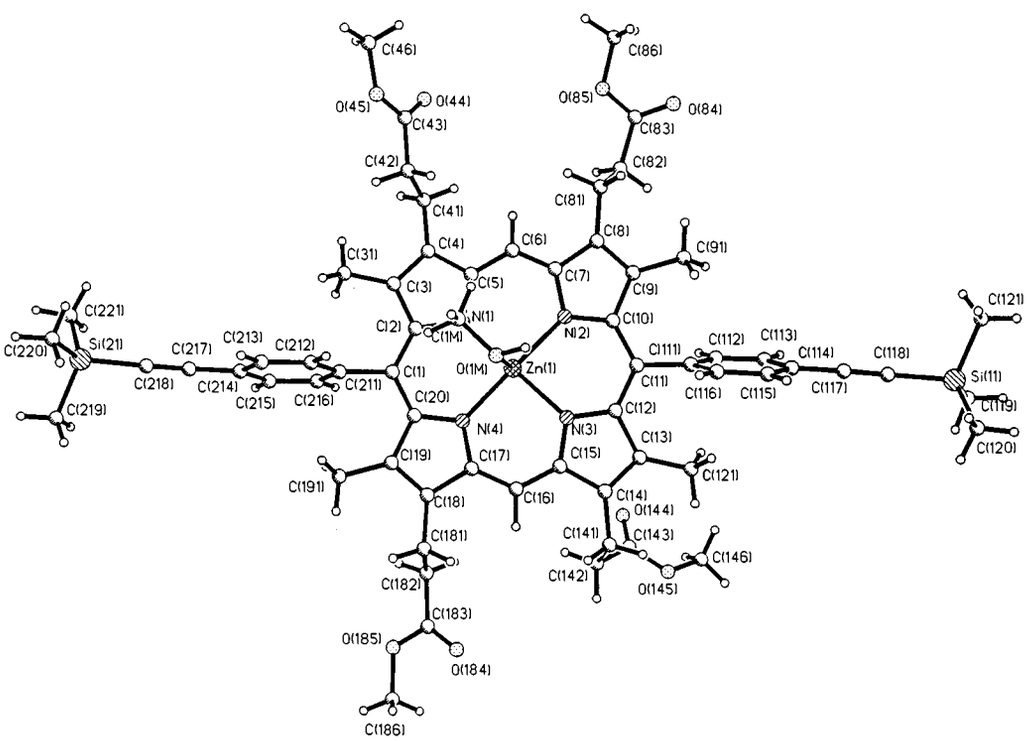

Fig. 4 Molecular structure of **6**·MeOH showing the distorted square pyramidal coordination. The Zn atom lies 0.173 Å above the N_4 square base which shows slight tetrahedral distortions from planarity [deviations N(1) −0.066, N(2) 0.067, N(3) −0.067, N(4) 0.066 Å]. Selected bond lengths to Zn (Å): N(1) 2.042(2), N(2) 2.068(2), N(3) 2.054(2), N(4) 2.055(2), O(1M) 2.249(2).

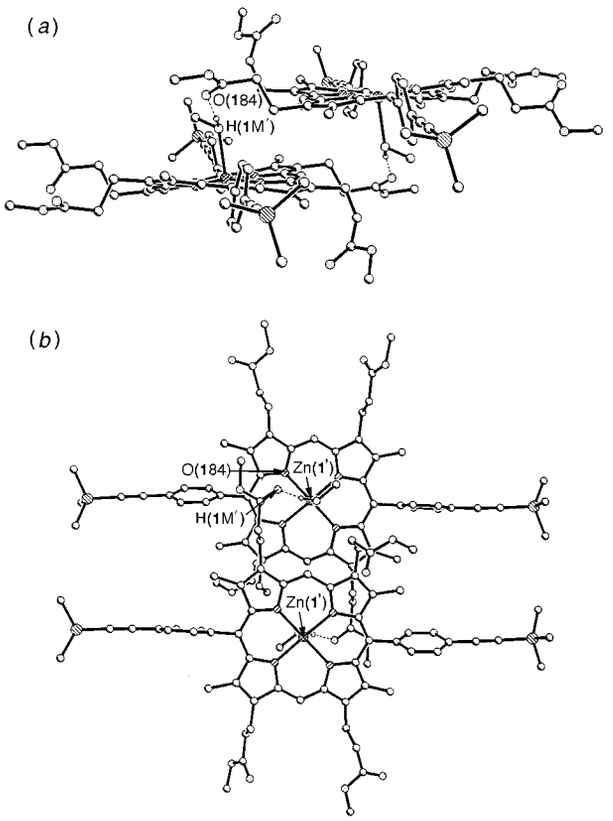

Fig. 5 (*a*) Side-view of the centrosymmetric hydrogen bonded dimeric unit in the crystal of **6**·MeOH [H(1M′) · · · O(184) 1.76 Å] showing how one ester side-arm on each molecule curls away to avoid close contact with the other porphyrin. (*b*) View onto both molecules of the dimeric unit showing the hydrogen bonding between the bound methanol and the carbonyl oxygen of a neighbouring porphyrin.

indeed offset with a disruption in the symmetry which renders all ester side-chains inequivalent. This is due not only to the horizontal offset of the molecules, but also in part to the 'curling' of one of the side-arms which appears to be hydrogen bonded to the zinc bound solvent molecule of an adjacent molecule, in order to accommodate a bound methanol of a porphyrin on an adjoining plane (Fig. 5). The weakly bound methanol is not observed in the ^{13}C CPMAS NMR spectrum, but might not be significant in the curling of the side-arm, as similar 'curling' is observed in the X-ray diffraction structure of a 1:2 DABCO–**6** complex, which is free of any methanol.[21] It is also likely that the 'flat' nature of the *para*-substituted aryl monomer **6** allows packing of a type not expected for the *meta*-substituted monomers, which might accommodate 'dimer' aggregates with the TMS acetylene arms pointing away from the porphyrin plane. The effect of this type of packing has been confirmed in the X-ray diffraction structure of the *meta*-substituted iodo monomer **3**, which exhibits splitting of the carbonyl signal in the ^{13}C CPMAS NMR spectrum, but no curling of the side-chains. In the X-ray diffraction structure of **3** (see latter), the asymmetric unit is defined by only half the molecule (Fig. 6). From the evidence described above for the other *meta*-substituted monomers (**1** and **2**), we would therefore expect two carbonyl resonances in the ^{13}C CPMAS NMR spectrum, which is exactly what is observed (at 169 and 172 ppm).

When the bulky TMS groups are replaced by less sterically demanding protons, as in the *para*-substituted de-protected monomer **7**, four carbonyl signals are again observed in the spectrum while the splitting of some of the other resonances in the spectrum become more pronounced than previously observed [Fig. 3(*b*)]. For example, the signal of the proton bearing *meso* carbon is now split by 6.3 ppm, in contrast to the lack

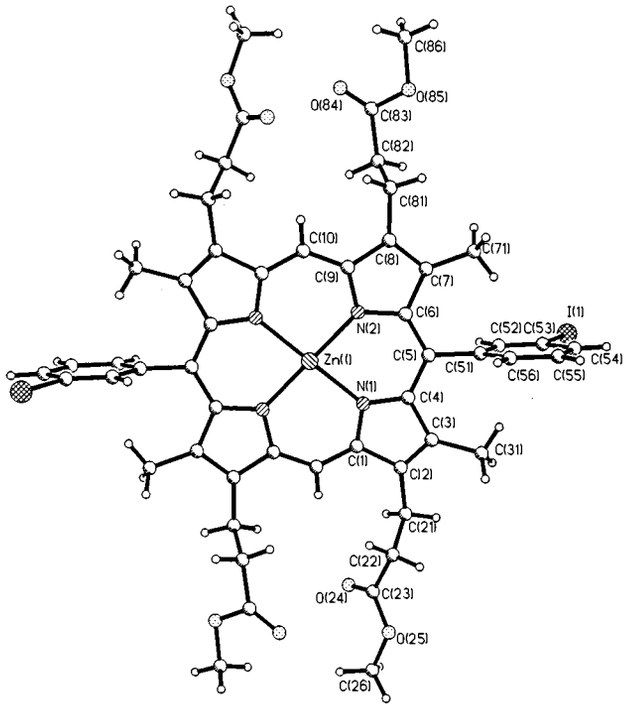

Fig. 6 Molecular structure of **3** showing the square planar coordination of the central zinc atom. Selected bond lengths to Zn (Å); N(1) 2.054(7) and N(2) 2.063(8) Å.

of observable splitting in most other monomers. The assignment of this *meso* signal was confirmed by a dipolar dephasing experiment,[22] which identifies carbon resonances according to the number of directly bonded protons.

For most of the *meta*-substituted monomers whose spectra were acquired, the possibility exists that there are both *cis* and *trans* forms (*i.e.* the position of the TMS acetylene groups relative to the porphyrin plane). In principle, this phenomenon could give rise to the observed splittings in the ^{13}C CPMAS spectra. Significantly though, for monomer **4**, there is only one possible isomeric form of the compound present (*trans*),‡,[23] yet splittings in the spectrum are observed. In fact, for this compound there is even a splitting of the aromatic methoxy signals [Fig. 2(*b*)], further suggesting that the observed splittings in this ^{13}C NMR spectrum are the result of the intermolecular stacking effects described above and not the possible 'conformers' of the molecule.

In the solution state, an interesting property is observed in the ^{1}H NMR spectra of the *meta*- and *para*-substituted aryl porphyrins. A concentrated solution of the relatively soluble *meta*-substituted TMS protected monomer **1** (*ca.* 30 mM), exhibits a splitting of the low field *meso*-resonance (*ca.* 0.01 ppm) in the ^{1}H NMR spectrum. This reduces to a sharp singlet as a function of sample dilution with an accompanying slight downfield shift, in addition to a change in the appearance of the aromatic resonances. In a coordinating solvent, such as deuteropyridine, the *meso*-signal of a concentrated solution stays sharp, with little variation in the chemical shift of the *meso*-signal or the appearance of the aromatic resonances as a function of dilution. Over a similar concentration range, the *meso*-resonance of the *para*-substituted TMS protected monomer **6** is observed as a relatively sharp singlet, with a similar downfield shift as a function of dilution (Fig. 7). The effect is significantly less evident when the free-base analogues are investigated. This observation may reflect a degree of aggregation in the solution state[24] of the metallated monomers which influences the rate of rotation about the porphyrin–aromatic

‡ The *trans*-isomer was isolated chromatographically and characterised by J. C. Prime from a *cis–trans* mixture.[23]

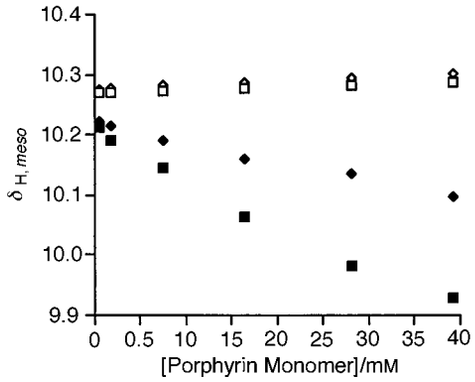

Fig. 7 Plot of the concentration of porphyrin monomer *versus* chemical shift of the *meso*-proton (400 MHz, $CDCl_3$) of the metallated and free-base monomers **1** and **6**: ◆, Zn(1); ■, Zn(6); ◇, H_2(1); □, H_2(6)

Table 1 Selected bond distances (Å) and bond angles (°) for **3** and **6**

	3	**6**
Zn(1)–N(1)	2.063(8)	2.042(3)
Zn(1)–N(1)[a]	2.064(8)	—
Zn(1)–N(2)	2.054(7)	2.068(3)
Zn(1)–N(2)[a]	2.054(7)	—
Zn(1)–N(3)	—	2.054(3)
Zn(1)–N(4)	—	2.055(3)
N(1)–Zn(1)–N(2)	87.3(3)	92.21(11)
N(1)–Zn(1)–N(4)	—	87.43(11)
N(1)–Zn(1)–N(2)[a]	92.7(3)	—
N(2)–Zn(1)–N(3)	—	86.58(11)
N(2)–Zn(1)–N(1)[a]	92.7(3)	—
N(3)–Zn(1)–N(4)	—	92.39(11)
N(1)–Zn(1)–N(3)	—	166.44(11)
N(1)–Zn(1)–N(1)[a]	180.0	—
N(2)–Zn(1)–N(4)	—	174.03(11)

Symmetry transformations used to generate equivalent atoms: [a] $-z+1, -y+1, -z$.

bond. In doing so, the appearance of the signals attributed to the *meta*-substituted monomer (in particular the split of the *meso*-proton and the change in the aromatic region) would be affected more than for the *para*-substituted analogue, though the variation in the chemical shift should be common to both molecules. Significantly, over the same concentration range, the ^{13}C NMR spectra appear essentially identical. Generally, this experiment cannot be applied to most porphyrins, which are sparingly soluble in most (non-coordinating) organic solvents. While the cause for this behaviour in solution is not clear, the correlation between the solid and solution state spectra for a limited number of molecules suggests that for the vast majority of porphyrin molecules, which are relatively insoluble, the solid state experiment may yield results consistent with the solution state experiments.

Crystal structures of 3 and 6

The X-ray structure determination of **6** confirms that the asymmetric unit in the solid state comprises the whole zinc porphyrin as the methanol complex **6**·MeOH (Fig. 4, Table 1), and that the overall C_i symmetry dictates that the four ester side-chains are inequivalent. Three of the ester side-arms adopt extended conformations but the overall lack of symmetry is emphasised by the fourth side-arm [on the pyrrole ring bearing N(3)] being curled away to avoid too close contact with the second porphyrin of a centrosymmetric dimer which exists in the crystal (Fig. 5). The dimer (and the off-set of the constituent monomer units) is dominated by the strong hydrogen bonding between the methanol ligands of the two linked porphyrin units [H(1M′)···O(184) 1.759 Å, Fig. 5(*a*)]. The two TMS–acetylene substituted phenyl rings are only approximately perpendicular to the N_4 plane (dihedral angles 73.4 and 83.6°). A similar solvent induced dimerisation was postulated by results of solution state NMR spectroscopy for a methyl pyrochlorophyllide *a* system,[25] and later confirmed by single crystal X-ray diffraction analysis.[26]

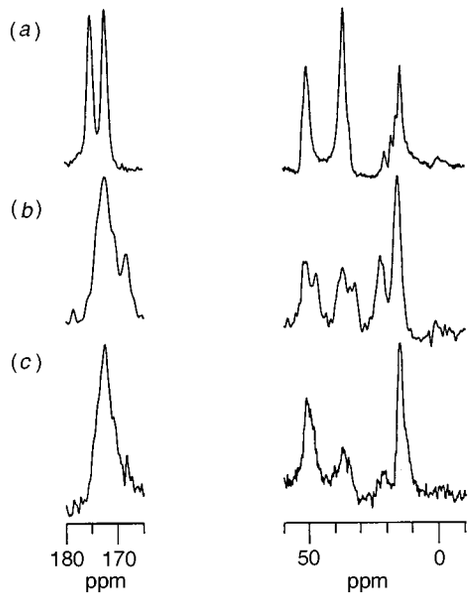

Fig. 8 Carbonyl (low field) and aliphatic (high field) regions of the ^{13}C CPMAS NMR (100.6 MHz) spectrum for a series of cyclic cavities: (*a*) Zn_2 2,2 non-rigid dimer **8**, (*b*) Zn_2 1,1 rigid dimer **9** and (*c*) Zn_2 2,2 rigid dimer **10**

The X-ray structure determination of **3** (Fig. 6) shows that the zinc atom (which is situated on an inversion centre) is exactly planar in its coordination; the Zn–N bond lengths of 2.054(7) and 2.063(8) Å are unremarkable (Table 1). All four ester side-arms extended away from the porphyrin, and there is no evidence of coordinated solvent in this structure which might dominate the offset of any two porphyrin units. The planes of the two iodinated aromatic rings are roughly perpendicular to the plane of the porphyrin, with a dihedral angle of 80.3°. Their rotation is restricted by steric clashes with the methyl groups on C(3) and C(9) of the porphyrins and there is significant disorder of the iodine atoms due to rotation about the aryl porphyrin bond.

Cyclic porphyrin oligomers

In contrast to the solid state spectra of most porphyrin monomers which exhibit a measurable splitting of the carbonyl signals, smaller splittings dependent on the rigidity of the cavity, were observed in the dimer molecules [**9** and **10**, Fig. 8(*a*)–(*c*)], while for the trimer cavity **11** no splitting was evident.

In the solid state spectrum of the collapsible zinc dimer [**8**, Fig. 8(*a*)], a splitting of the carbonyl signal was apparent. This is a non-rigid system and the porphyrin rings have the capacity to stack intramolecularly 'off-centre' with respect to one another [Fig. 9(*b*)], in a similar manner to the off-centre stacking described earlier for the porphyrin monomers [Fig. 9(*a*)].

The ^{13}C CPMAS NMR spectrum of the small, rigid zinc dimer **9** displays several split signals [Fig. 8(*b*)]. The magnitude of the carbonyl splitting (4.0 ppm) is one of the largest measured in this study, yet the rigidity of the acetylene straps between molecular sub-units ensures that no intramolecular offset is possible. However, intermolecular offset stacking is viable. It may be argued that as the molecules are small, they may pack efficiently, resulting in enhanced ring current interactions with the functional groups of adjacent dimers (and resulting in large signal splittings).

The larger acetylenic dimer **10** is, like the 1,1 analogue, a rigid system where intramolecular offsetting of porphyrin rings is

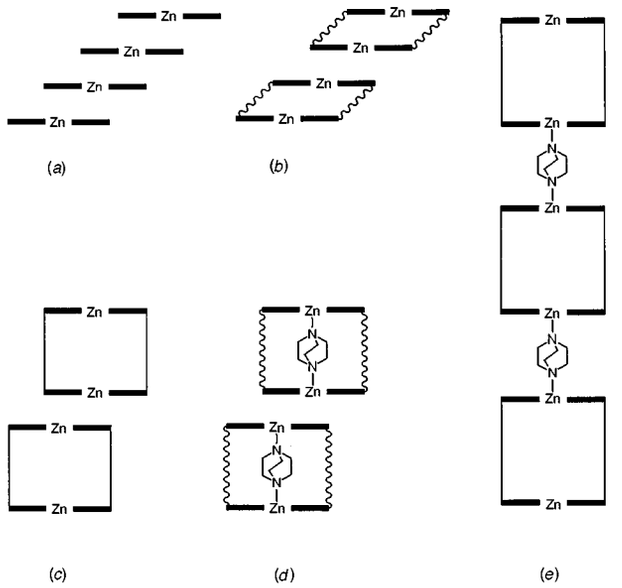

Fig. 9 Possible π–π stacking interactions for (*a*) a monomer, (*b*) a non-rigid dimer, (*c*) a rigid dimer; the dimer may be the 1,1 dimer or the larger 2,2 analogue, (*d*) a non-rigid (floppy) dimer with DABCO bound inside the cavity and (*e*) a rigid dimer with DABCO bound 'outside' the cavity

not possible. For this compound, splitting of the carbonyl signal is not detected in the ^{13}C CPMAS NMR spectrum, but small splittings for some of the high field resonances are evident [Fig. 8(*c*)]. An explanation for this observation might be that although an intermolecular offset stacking arrangement is likely [Fig. 9(*c*)], the larger molecules are not so closely packed in the solid state and as a result, the ring current effects are diminished.

When the ^{13}C CPMAS NMR spectra of rigid and non-rigid zinc porphyrin trimers were acquired (**11** and **12**, respectively), no carbonyl splitting was observed. Any carbonyl splitting that may be present was too small to resolve, although it should be noted that the linewidths of the spectra for the non-rigid cavities were comparable to those for the rigid analogues. In the solution state, the non-rigid (floppy) trimer **12** is known to be a mixture of four rapidly exchanging conformations[27] and the lack of observable signal splitting in the ^{13}C CPMAS NMR spectrum reflects the fact that with three porphyrin units per molecule, intramolecular pairing of porphyrins; to stack off-centre (in an ordered manner) as seen for the non-rigid dimer, is not possible. Intermolecular stacking, even if offset, would be such that any ring current effects would be very small as the molecules are so large that they cannot efficiently pack. Therefore for trimers, whether the system is rigid or not, no resonance splitting in the ^{13}C CPMAS NMR spectrum is observed.

Host–guest complexes

Comparison of the ^{13}C CPMAS solid state NMR spectra of various porphyrin cavities, both with and without small coordinated molecules, provides valuable empirical information about the host–guest interactions of porphyrins and small molecules in the solid state. The spectrum of the 'ternary complex' resulting from the complexation of diaminobicyclooctane (DABCO) to two zinc monomers **13** contained a split carbonyl signal and a split methoxy carbon signal [Fig. 10(*a*)]. These splittings can be attributed to the intermolecular offset stacking of molecules, described earlier. The porphyrin-to-porphyrin distance of the resulting adduct is comparable to that in the 1,1 dimer **9**, and close packing of molecules in the solid state might be predicted. This is reflected in the magnitude of the splitting of the carbonyl resonance (3.5 ppm). From solution state ^{13}C NMR spectra, one would expect DABCO to resonate at

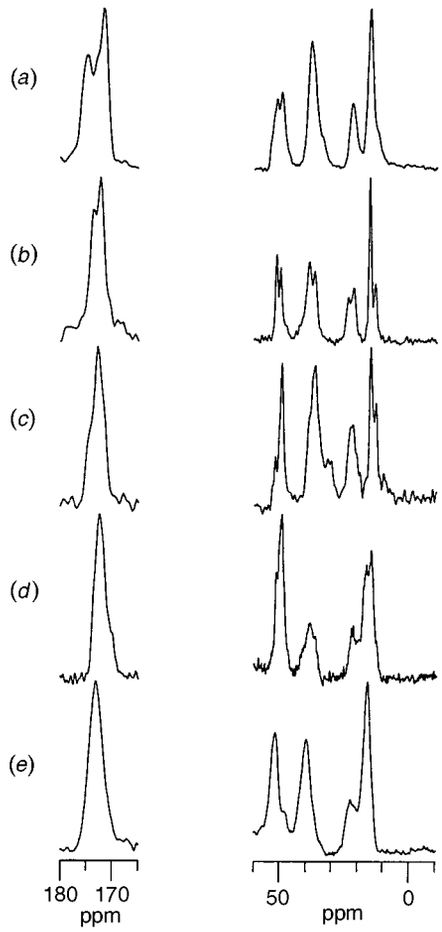

Fig. 10 Carbonyl (low field) and aliphatic (high field) regions of the ^{13}C CPMAS NMR (100.6 MHz) spectrum for a series of host–guest complexes: (*a*) 2:1 monomer (1):DABCO 'sandwich' complex **13**, (*b*) 1:1 1,1 rigid dimer **9**–DABCO complex **14**, (*c*) 1:1 2,2 non-rigid (floppy) dimer **8**–DABCO complex **15**, (*d*) 1:1 2,2 rigid dimer **10**–BiPy complex **16**, (*e*) 1:1 2,2 rigid dimer **10**–DABCO complex **17**. Possible structures of the respective complexes are also shown.

approximately 38 ppm, but should this be the case in the solid state spectrum, it would be obscured by an ester side-chain methylene signal at the same chemical shift value. It should be noted that the cavity size of the Zn_2 1,1 dimer is complementary for a DABCO molecule (from solution state NMR competition studies)[28] and DABCO binds exclusively inside the cavity. As a result, in the ^{13}C CPMAS solid state NMR spectrum of the adduct **14** [Fig. 10(*b*)], the carbonyl signal is split, as are other side-chain signals due to the intermolecular offset stacking and close molecular packing; similar to the case for the ligand-free 1,1 dimer.

The split carbonyl resonance evident in the spectrum of the ligand-free, non-rigid (floppy) dimer **8** was absent in the ^{13}C CPMAS solid state NMR spectrum of the 2,2 floppy dimer DABCO complex **15** [Fig. 10(*c*)], although the carbonyl peak was slightly unsymmetrical. Coordination of DABCO inside this more flexible dimer cavity is probable, despite it being too large, as the flexibility of the system enables complexation *via* relaxation of the butyl chains connecting the porphyrin rings [Fig. 9(*d*)].[27] The bound DABCO therefore constrains the system, preventing the two porphyrin sub-units from lying off centre with respect to each other. Signals due to the side-chain groups and the ring methyl resonances at lower chemical shift values are split, again as a consequence of intermolecular rather than intramolecular offset stacking.

A similar effect was observed in the formation of a 4,4′-bipyridyl (BiPy) 2,2 rigid dimer complex [**16**, Fig. 10(*d*)], where the bipyridyl molecule (used as a positive template in the syn-

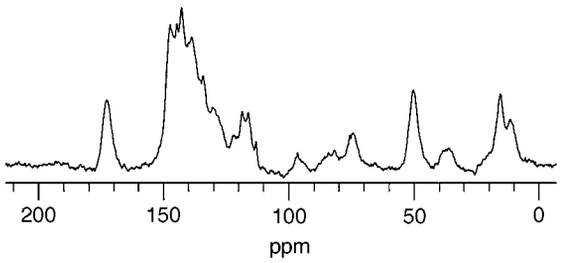

Fig. 11 ^{13}C CPMAS NMR (100.6 MHz) spectrum of Zn_4 tetramer-Py_4P adduct **18**

thesis of the host)[29] is the ideal size to fit into the cavity of the rigid dimer. The ^{13}C CPMAS NMR spectrum of this adduct is similar to that of the ligand-free rigid dimer, in that no carbonyl splitting was resolved, although splittings were observed for the high field resonances as a result of intermolecular stacking effects. This is entirely consistent with the bipyridyl guest binding inside the host.

Based on the above results, it was predicted that the ^{13}C CPMAS NMR spectrum of the 2,2 rigid dimer DABCO adduct **17** would show no splittings for either the carbonyl or higher field resonances (methylene and methyl). CPK models indicate that DABCO is too small to fit 'efficiently' into the rigid dimer cavity, but can coordinate externally, between pairs of dimers to form a linear coordination polymer [Fig. 9(*e*)].[30] The spectrum of **18**, [Fig. 10(*e*)] confirms this prediction, with no splittings evident for either the carbonyl or high field signals; in the solution state, there is evidence for the competing formation of a single dimer with DABCO binding as a monodentate, or loose bidentate, inside the cavity, perhaps as an equilibrium mixture, although this was the minor product.

A ^{13}C CPMAS NMR spectrum of the zinc tetramer-5,10,15,20-tetra(4-pyridyl)porphyrin (Py_4P) adduct (**18**, Fig. 11) was also acquired. For this compound, an X-ray crystal structure was previously available for direct comparison.[13] It was also the only compound examined for which inequivalence of ring methyl and ester side-chain groups within a single molecule is observed; this inequivalence is a result of the symmetry of the complex. In the solution state ^{13}C NMR spectrum of this compound, inequivalent ring methyl carbons were split by 0.8 ppm. For the ^{13}C CPMAS NMR spectrum however, this split was 4.0 ppm, which is much too large to be accounted for by intramolecular inequivalence. Examination of the crystal structure reveals, that although the molecules stack vertically in mutually opposed pairs, molecules that are adjacent to each other horizontally, are offset in a manner similar to that known for planar porphyrin monomers. As a consequence, the observed ring methyl splitting can be rationalised in terms of intermolecular effects arising from the ring current of one molecule affecting an adjacent one. No splitting was evident for the carbonyl signal in the spectrum but it is known from the crystal structure that this group is in rapid motion and hence only an average signal is observed; deconvolution of the resonance suggests that it consists of two peaks in a ratio of 1 : 1. A comparison of the crystal structure and the spatial distribution of molecules derived from the ^{13}C CPMAS NMR spectrum of the tetramer, indicates that the interpretation of the solid state spectrum provides quite an accurate method of predicting the 'packing' in the solid state and in the absence of suitable crystals for X-ray diffraction analysis, offers a valuable complement to high resolution, solution state NMR spectroscopy.

Conclusions

This investigation of a series of metalloporphyrin monomers, oligomers and host–guest complexes by ^{13}C CPMAS NMR spectroscopy has shown that the technique appears to be a reliable method for obtaining information on crystal packing in the solid state, as the results obtained are in good agreement with the limited number of known crystal structures of the porphyrins under investigation. In particular, the X-ray structure reported for **3** and **6**, and the corresponding ^{13}C CPMAS NMR spectra, provide the most convincing evidence yet for the interpretation of packing based on two independent solid state methods. In principle, this technique could be extended to any system for which obtaining good quality crystals for X-ray diffraction studies is difficult. The appearance of the spectra presented in this study can be accounted for by invoking π–π stacking arguments, in addition to identification of the nature of the asymmetric unit, though one may follow from the other. Furthermore, as in the case of the linear network formed between the rigid dimer and DABCO, we have demonstrated the ability of CPMAS NMR spectroscopy to confirm predictions made about molecular stacking in the solid state.

Experimental

^{1}H–^{13}C cross-polarisation magic-angle spinning (CPMAS) NMR spectra of a series of zinc porphyrin monomers **1**,[31] **2**,[31] **3**,[32] **4**,[23] **5**,[18] **6** and **7**, dimers **8**,[27] **9**[28] and **10**,[31] trimers **11**,[31] **12**[27] and host–guest complexes§ **13**,[21] **14**,[28] **15**,[27] **16**,[29] **17**[30] and **18**[13,33] were recorded using the total sideband suppression (TOSS) pulse sequence[34] on a Chemagnetics CMX-400 spectrometer operating at 100.6 MHz (9.4 T) with 4 ms (ambient temperature) ^{1}H 90° pulse, 4 ms contact times and 10 s recycle delays. Samples of between 50–100 mg were spun in a 4 mm rotor at 4500 ± 5 Hz. Complexes were obtained by mixing stoichiometric quantities of host and guest in a minimum volume of solvent (*ca.* 1–2 ml), stirring for 5 min and then evaporating the solvent under a stream of argon or nitrogen. The product was then collected as a powder. The Hartmann–Hahn condition[35] was established on hexamethylbenzene using 4 ms contact times and 4 s recycle delays. ^{13}C NMR chemical shifts are given in ppm referenced from external tetramethylsilane (TMS). The number of data points used for each spectrum was 1 K, with 4 K zero filling and line broadening of the order 10–40 Hz employed. The number of transients per experiment varied between 500–5000, depending on the amount and the signal-to-noise ratio of each individual sample. Solution state ^{13}C NMR spectra (with CPD proton decoupling) were recorded on a Bruker AM 400 spectrometer operating at 100.6 MHz at ambient temperature, typically as a $CDCl_3$ solution (solvent passed through a short, basic alumina plug, to remove water and acid).

The spectroscopic properties of **1**[31] (in the solution state) shown in Fig. 1(*b*) and used in the preparation of the cyclic hosts, are reported below (for reference). For the series of *meta*-substituted porphyrins investigated, the change in chemical shift for a particular resonance in a similar chemical environment is negligible.

δ_H(250 MHz, $CDCl_3$) 0.28 (18 H, s, $SiMe_3$), 2.45 (12 H, s, Me), 3.08 (8 H, t, *J* 7.7, CH_2CH_2COOMe), 3.67 (12 H, s, MeO), 4.20 (8 H, t, *J* 7.7, CH_2CH_2COOMe), 7.68–8.18 (8 H, m, aryl-*H*), 10.02 (2 H, s, *meso*-*H*); δ_C(100 MHz, $CDCl_3$) 0.0 ($SiMe_3$), 15.6 (Me), 21.8 (CH_2CH_2COOMe), 36.9 (CH_2CH_2COOMe), 51.7 (MeO), 94.7 (C≡*C*–$SiMe_3$), 97.3 (*meso*-C), 105.1 (*C*≡C–$SiMe_3$), 118.7 (*meso*-aryl), 122.7 (aryl-C≡C), 127.6, 132.0, 133.1 and 136.3 (aryl-H), 139.0, 141.4, 145.9 and 147.5 (pyrrole), 143.5 (aryl-porph), 173.5 (COOMe).

4-(2-Trimethylsilylethynyl)benzaldehyde (used in the following step) was prepared (white solid from recrystallisation with

§ Complexes were prepared by addition (stoichiometric) of the appropriate guest of known concentration, to a solution of porphyrin monomer **1** or hosts **7**–**9**. The mixtures were allowed to stir for 30 min and the solvent (CH_2Cl_2 or $CHCl_3$) allowed to evaporate, affording the product as red powders/films.

cold hexane) *via* the Pd-mediated coupling[36] of 4-bromobenzaldehyde and trimethylsilylethyne, following a previously reported synthesis of 3-(2-trimethylsilylethynyl)benzaldehyde.[37] δ_H(250 MHz, $CDCl_3$) 0.24 (9 H, s, $SiMe_3$), 7.56 and 7.77 (2 × 2 H, 2 × d, *J* 8.3, aryl-*H*); δ_C(63 MHz, $CDCl_3$) 0.0 ($SiMe_3$), 99.0 and 103.8 (C≡*C*-$SiMe_3$), 129.3 and 135.6 (aryl-C), 129.4 and 132.4 (aryl-H), 191.3 (CO).

Preparation of 6. Palladium on carbon (200 mg, 10%) was added to a solution of 5,5′-bis(benzyloxycarbonyl)-3,3′-bis-(2-methoxycarbonylethyl)-4,4′-dimethyl-2,2′-dihydropyrrin[38] (5.00 g, 8.13 mmol) in THF (100 ml, distilled *ex*. $LiAlH_4$) containing 1% triethylamine. The mixture was de-oxygenated (three cycles of exposing to vacuum and hydrogen gas) and stirred under hydrogen for 3 h. The catalyst was filtered and the filtrate evaporated before drying under vacuum for 3 h. The residue was cooled (0 °C, ice bath) and degassed TFA (40 ml, three freeze–thaw cycles) added *via* canula under argon. The mixture was stirred at 0 °C for 20 min and allowed to stir at 20 °C for a further 20 min. Periodically, the reaction vessel was evacuated and Ar introduced in order to remove CO_2, and in the process reduce the solvent volume to half. At this stage, the dark orange solution was cooled to −25 °C (ice, dry-ice, acetone). A de-oxygenated solution (three cycles of exposing to vacuum and argon gas) of 4-(trimethylsilylethynyl)benzaldehyde (1.62 g, 8.02 mmol) in methanol (40 ml) was added to the cold solution of the dipyrrolylmethane *via* canula. The mixture was left to stir for 2 h at −20 °C. The cold bath was removed and 2,3-dichloro-5,6-dicyano-1,4-benzoquinone (DDQ) (2.76 g, 12.01 mmol) was added, followed with $CHCl_3$ (5 ml) and the mixture stirred for 5 min. CH_2Cl_2 (300 ml) was then added and the dark solution washed with $NaHCO_3$ (saturated solution, 2 × 300 ml, **CAUTION:** exothermic reaction). The organic solution was washed with H_2O (2 × 400 ml), the solvent removed and the dark residue recrystallised by layered addition of CH_3OH onto a concentrated CH_2Cl_2 solution of the crude porphyrin mixture. The resulting fibrous brown solid was filtered (two crops) and dried *in vacuo* to yield the free-base product (1.20 g, 28%).

Free-base monomer H_2-6. δ_H(400 MHz, $CDCl_3$) −2.44 (2 H, br s, N-*H*), 0.43 (18 H, s, $SiMe_3$), 2.52 (12 H, s, Me), 3.16 (8 H, t, *J* 7.8, CH_2CH_2COOMe), 3.68 (12 H, s, MeO), 4.36 (8 H, t, *J* 7.8, CH_2CH_2COOMe), 7.89 and 8.01 (2 × 4 H, 2 × d, *J* 7.8, aryl-H), 10.28 (2 H, s, *meso*-H); δ_C(100 MHz, $CDCl_3$) 0.1 ($SiMe_3$), 14.9 (Me), 21.9 (CH_2CH_2COOMe), 36.9 (CH_2CH_2COOMe), 51.6 (MeO), 95.4 (C≡*C*–$SiMe_3$), 96.7 (*meso*-C), 105.1 (*C*≡C–$SiMe_3$), 117.7 (*meso*-aryl), 123.4 (*aryl*-C≡C), 131.4 and 132.7 (aryl-H), 137.2, 141.1, 141.4 and 144.7 (pyrrole), 142.2 (*aryl*-porph), 173.5 (*C*OOMe).

Zinc monomer Zn–6. Metallation of the free-base monomer was achieved by dissolving in $CHCl_3$ and adding excess zinc acetate dihydrate with a small amount of CH_3OH. The resulting solution was allowed to stir for 30 min or until the reaction was deemed complete by TLC ($CHCl_3$). The red solution was washed with water, the solvent removed and the residue recrystallised by layered addition of CH_3OH onto a concentrated CH_2Cl_2 solution of the porphyrin. The resulting red solid was filtered (two crops) and dried *in vacuo* to afford **6** in quantitative yield. δ_H(400 MHz, $CDCl_3$) 0.40 (18 H, s, $SiMe_3$), 2.46 (12 H, s, Me), 3.12 (8 H, t, *J* 7.9, CH_2CH_2COOMe), 3.65 (12 H, s, MeO), 4.30 (8 H, t, *J* 7.9, CH_2CH_2COOMe), 7.86 and 8.00 (2 × 4 H, 2 × d, *J* 8.0, aryl-*H*), 10.18 (2 H, s, *meso*-*H*); δ_C(100 MHz, $CDCl_3$) 0.1 ($SiMe_3$), 15.4 (Me), 21.7 (CH_2CH_2COOMe), 36.9 (CH_2CH_2COOMe), 51.7 (MeO), 95.2 (C≡*C*–$SiMe_3$), 97.2 (*meso*-C), 105.3 (*C*≡C–$SiMe_3$), 118.8 (*meso*-aryl), 123.2 (*aryl*-C≡C), 131.3, 133.0 (*aryl*-H), 138.8, 141.3, 145.7 and 147.3 (pyrrole), 143.7 (*aryl*-porph), 173.5 (COOMe).

Preparation of 7. Quantitative removal of the TMS groups was achieved by addition of tetrabutylammonium fluoride (2 equivs., as a 1 M solution in THF) to a CH_2Cl_2 solution of **6**. The mixture was allowed to stir at room temperature until no starting material was detected by TLC ($CHCl_3$, *ca*. 1 h). Two spatula of $CaCl_2$ were then added, the mixture stirred for 2 min and finally washed with H_2O (2 × 50 ml). The organic solution was concentrated, layered with MeOH and the porphyrin product filtered and dried (*in vacuo*). δ_H(400 MHz, $CDCl_3$) 2.46 (12 H, s, Me), 3.11 (8 H, t, *J* 8.0, CH_2CH_2COOMe), 3.37 (2 H, s, C≡C*H*), 3.67 (12 H, s, MeO), 4.31 (8 H, t, *J* 8.0, CH_2CH_2COOMe), 7.89 and 8.03 (2 × 4 H, 2 × m, aryl-*H*), 10.17 (2 H, s, *meso*-*H*); δ_C(100 MHz, $CDCl_3$) 15.5 (Me), 21.9 (CH_2CH_2COOMe), 36.9 (CH_2CH_2COOMe), 51.7 (MeO), 78.2 (C≡*C*–H), 83.6 (*C*≡C–H), 97.3 (*meso*-C), 1189 (*meso*-aryl), 122.2 (*aryl*-C≡C), 131.4, 133.1 (*aryl*-H), 138.6, 141.3, 145.7 and 147.3 (pyrrole), 143.6 (*aryl*-porph), 173.5 (COOMe).

Table 2 Crystallographic data for **3** and **6**

	3	**6**
Formula	$C_{52}H_{50}I_2N_4O_8Zn$	$C_{63}H_{72}N_4O_9Si_2Zn$
M_r	1178.14	1150.80
Crystal	Triclinic	Triclinic
Space group	$P\bar{1}$ (No. 2)	$P\bar{1}$ (No. 2)
a/Å	8.997(3)	12.618(1)
b/Å	11.393(4)	14.317(2)
c/Å	11.735(4)	17.915(2)
α/°	88.30(2)	81.892(9)
β/°	90.12(2)	70.009(6)
γ/°	74.93(2)	85.933(6)
U/Å^3	1160.9(7)	3010.1(6)
Z	1	2
F(000)	1180	1216
D_c/g cm^{-3}	1.685	1.270
λ/Å	0.710 69	154 178
Crystal size/mm	0.04 × 0.02 × 0.01	0.16 × 0.40 × 0.40
μ/mm^{-1}	(Mo-Kα) 1.920	(Cu-Kα) 1.420
Reflections	4977	9335
No. unique	2293	8016
R_{int}	0.0570	0.0553
T/K	100(2)	173(2)

X-Ray crystallography

Crystal data for 3. Data collection. Data were collected on a poor quality red crystal (crystallised from CH_2Cl_2–CH_3OH) of approximate dimensions 0.04 × 0.02 × 0.01 mm using a Mar-Research 18 cm Image Plate detector mounted on the protein crystallography beamline at the Sincrotrone Elettra, Trieste, Italy, fitted with an Oxford Cryosystems Cryostream low temperature device (Table 2). 4977 reflections were collected in the *θ* range 2.34–20.83° using the Arndt–Wonacott oscillation method; 15 images each with a 12° oscillation range were collected with a crystal to detector distance of 100 mm, using the constant count option in the data collection software. The geometry of the beamline made high angle data collection impossible, but the wavelength of the X-rays was tuned to 0.710 69 Å to approximate to Mo-Kα radiation and also to enable some higher angle data to be collected. The data were processed *via* standard macromolecular techniques[39] and corrected for Lorentz and polarisation effects, but not for absorption,[40] and merged to give 2293 unique reflections (R_{int} = 0.057).

Structure solution and refinement. The structure was solved by direct methods and all non-hydrogen atoms located from subsequent difference Fourier syntheses. The halogeno-substituted aromatic rings were found to be disordered between two orientations, shown by the iodines on the *meta*-positions on the rings having site occupancy factors in the approximate ratio 4.7 : 1. This resulted in a difficulty with the refinement of C(55), which was bonded partly to a 0.175 occupancy iodine, and partly to a hydrogen with occupancy 0.825. All non-hydrogen atoms [except C(55)] were assigned anisotropic displacement parameters and refined using full matrix least squares on F_o^2.[41] The hydrogen atoms were included in calculated positions; during refinement they were allowed to ride on their parent

carbon atoms and assigned isotropic displacement parameters based on simple multiples of their parent atoms U(equiv.) values. The refinement converged at $wR2 = 0.2574$ and $R1 = 0.0995$ (all 2293 data, $wR2 = 0.2429$ and $R1 = 0.0965$ *for 2254 data* $I > 2\sigma(I)$, goodness of fit (S) on $F^2 = 1.265$, for 305 parameters with 33 geometrical restraints. Weights of $1/[\sigma^2(F_o^2) + (0.0582P)^2 + 32.45P]$, where $P = (\max[F_o^2, 0] + 2F_c^2)/3$ were assigned to the individual reflections.

Crystal data for 6. Data collection. Data were collected on a purple crystal (crystallised from CH_2Cl_2–CH_3OH) of dimensions 0.16 × 0.40 × 0.40 mm using a Siemens P4 diffractometer equipped with a Siemens LT2 low temperature device (Table 2). No significant decay in the intensity of three standard reflections measured after every 100 reflections was observed. 9335 reflections were collected in the θ range 2.65–56.75°. The data were corrected for Lorentz and polarisation factors but not for absorption and merged giving 8016 unique reflections ($T_{int} = 0.0553$).

Structure solution and refinement. The structure was solved by direct methods and all non-hydrogen atoms were located from subsequent difference Fourier syntheses. All non-hydrogen atoms were assigned anisotropic thermal parameters and refined using full-matrix least squares on F_o^2.[41] The hydrogen atoms were included at calculated positions with C–H bond distances of 0.95 and 0.98 Å for the aromatic and methyl groups, respectively. The hydroxylic hydrogen of the coordinated methanol and the methine hydrogens were located from Fourier-difference syntheses. During refinement, all the hydrogens were allowed to ride on their parent atom, but positional parameters of the directly located hydrogens were not refined. The refinement convergence at $wR2 = 0.1272$ (all data) for 8016 data {$R1 = 0.464$, [for 6948 data $I = 2\sigma(I)$], goodness-of-fit (S) on $F^2 = 1.024$} and 727 parameters. Weights of $1/[\sigma^2(F_o)^2 + (0.0758P) + 2.4091P]$, where $P = \{\max[(F_o)^2, 0] + (F_c)^2\}/3$ were assigned to the individual reflections.

Full crystallographic details, excluding structure factor tables, have been deposited at the Cambridge Crystallographic Data Centre (CCDC). For details of the deposition scheme, see 'Instructions for Authors', *J. Chem. Soc.*, *Perkin Trans. 2*, available *via* the RSC Web page (http://www.rsc.org/authors). Any request to the CCDC for this material should quote the full literature citation and the reference number 188/118.

Acknowledgements

We thank J. C. Prime, Z. Clyde-Watson, D. W. J. McCallien and S. Fanni for the supply of some samples, C. J. Anderson, B. K. Hunter and C. A. Hunter for making available unpublished CPMAS spectra (1986–89) and N. Feeder for help producing the X-ray plots. Financial support from the SERC/EPSERC (N. B.), the European Union Human Capital and Mobility Program (A. V. F.), the Newton Trust, the University of Waikato and Royal Society of New Zealand (M. R. P.) is gratefully acknowledged. Finally, we thank an anonymous referee for helpful and perceptive comments on the first version of this paper.

References

1 (*a*) A. Pines, M. G. Gibby and J. S. Waugh, *J. Chem. Phys.*, 1973, **59**, 569; (*b*) E. R. Andrew, *Progr. Nucl. Magn. Reson. Spectrosc.*, 1971, **8**, 1; (*c*) J. Schaeffer and E. O. Stejskal, *J. Am. Chem. Soc.*, 1976, **98**, 1031.
2 C. S. Yannoni, *Acc. Chem. Res.*, 1982, **15**, 201.
3 See for example, C. A. Fyfe, *Solid State NMR for Chemists*, CFC Press, Ontario, 1983.
4 See for example, (*a*) J. K. M. Sanders and B. K. Hunter, *Modern NMR Spectroscopy. A Guide to Chemists*, Oxford University Press, Oxford, 2nd edn., 1993; (*b*) D. H. Williams and I. Fleming, *Spectroscopic Methods in Organic Chemistry*, McGraw-Hill, Maidenhead, 5th edn., 1995.
5 (*a*) *Porphyrins and Metalloporphyrins*, ed. K. Smith, Elsevier, Amsterdam, 1975; (*b*) *The Porphyrins*, ed. D. Dolphin, Academic Press, New York, 1979, vols. 6 and 7.
6 See for example, (*a*) M. J. Crossley, M. M. Harding and S. Sternhell, *J. Am. Chem. Soc.*, 1986, **108**, 3608; (*b*) M. J. Crossley, L. D. Field, M. M. Harding and S. Sternhell, *J. Am. Chem. Soc.*, 1987, **109**, 2335, and references cited therein; (*c*) M. Schlabach, H. Limbach, E. Bunnenberg, A. Y. L. Shu, B. R. Tolf and C. J. Djerassi, *J. Am. Chem. Soc.*, 1993, **115**, 4554.
7 L. Frydman, A. C. Olivieri, L. E. Díaz, A. Valasinas and B. Frydman, *J. Am. Chem. Soc.*, 1988, **110**, 5651.
8 L. Frydman, A. C. Olivieri, L. E. Díaz, B. Frydman, I. Kustanovich and S. Vega, *J. Am. Chem. Soc.*, 1989, **111**, 7001.
9 H. H. Limbach, J. Henning, R. Kendrick and C. S. Yannoni, *J. Am. Chem. Soc.*, 1984, **106**, 4059.
10 R. J. Butcher, G. B. Jameson and C. B. Storm, *J. Am. Chem. Soc.*, 1985, **107**, 2978.
11 B. Wehrle, H. H. Limbach, M. Köcher, O. Ermer and E. Vogel, *Angew. Chem.*, *Int. Ed. Engl.*, 1987, **26**, 934.
12 H. L. Anderson, A. Bashall, K. Henrick, M. McPartlin and J. K. M. Sanders, *Angew. Chem.*, *Int. Ed. Engl.*, 1994, **33**, 429.
13 S. Anderson, H. L. Anderson, A. Bashall, M. McPartlin and J. K. M. Sanders, *Angew. Chem.*, *Int. Ed. Engl.*, 1995, **34**, 1096.
14 (*a*) R. J. Abraham, C. J. Medforth, K. M. Smith, D. A. Goff and D. J. Simpson, *J. Am. Chem. Soc.*, 1987, **109**, 4786; (*b*) R. J. Abraham, G. R. Bedford, D. McNeille and B. Wright, *Org. Magn. Reson.*, 1980, **14**, 418; (*c*) R. J. Abraham and C. J. Medforth, *Magn. Reson. Chem.*, 1987, **25**, 432; (*d*) R. J. Abraham, K. M. smith, D. A. Goff and F. W. Bobe, *J. Am. Chem. Soc.*, 1985, **107**, 1085.
15 C. A. Hunter and J. K. M. Sanders, *J. Am. Chem. Soc.*, 1990, **112**, 5525.
16 D. L. VanderHart, W. L. Earl and A. N. Garroway, *J. Magn. Reson.*, 1981, **44**, 361.
17 P. Leighton, J. A. Cowan, R. J. Abraham and J. K. M. Sanders, *J. Org. Chem.*, 1988, **53**, 733.
18 D. W. J. McCallien, Ph.D. Thesis, University of Cambridge, 1996.
19 W. Jentzen, M. C. Simpson, J. D. Hobbs, X. Song, T. Ema, Y. Nelson, C. J. Medforth, K. M. Smith, M. Veyrat, M. Mazzanti, R. Ramasseul, J.-C. Marchon, T. Takeuchi, W. A. III Goddard and J. Shelnutt, *J. Am. Chem. Soc.*, 1995, **117**, 11 085.
20 M. O. Senge and K. M. Smith, *J. Chem. Soc.*, *Chem. Commun.*, 1994, 923.
21 N. Bampos and J. K. M. Sanders, unpublished results.
22 S. J. Opella and M. H. Frey, *J. Am. Chem. Soc.*, 1979, **101**, 5855.
23 J. C. Prime, Ph.D. Thesis, University of Cambridge, 1996.
24 *The Porphyrins*, ed. D. Dolphin, Academic Press, New York, 1979, vol. 4, p. 12.
25 R. A. Abraham, A. E. Rowan, D. A. Goff, K. E. Mansfield and K. M. Smith, *J. Chem. Soc.*, *Perkin Trans. 2*, 1989, 1633.
26 H.-C. Chow, R. Sterlin and C. E. Strouse, *J. Am. Chem. Soc.*, 1975, **97**, 7230.
27 N. Bampos, V. Marvaud and J. K. M. Sanders, *Chem. Eur. J.*, in the press.
28 A. Vidal-Ferran, Z. Clyde-Watson, N. Bampos and J. K. M. Sanders, *J. Org. Chem.*, 1997, **62**, 240.
29 S. Anderson, H. L. Anderson and J. K. M. Sanders, *J. Chem. Soc.*, *Perkin Trans. 1*, 1995, 2231.
30 N. Bampos, R. S. Wylie, A. E. Rowan and J. K. M. Sanders, unpublished results.
31 S. Anderson, H. L. Anderson and J. K. M. Sanders, *J. Chem. Soc.*, *Perkin Trans. 1*, 1995, 2247.
32 (*a*) A. Vidal-Ferran, C. M. Müller and J. K. M. Sanders, *J. Chem. Soc.*, *Chem. Commun.*, 1994, 2657; *ibid.*, 1996, 1849; (*b*) A. Vidal-Ferran, N. Bampos and J. K. M. Sanders, *Inorg. Chem.*, in the press.
33 S. Anderson, H. L. Anderson and J. K. M. Sanders, *J. Chem. Soc.*, *Perkin Trans. 1*, 1995, 2255.
34 J. Schaefer, M. D. Sefcik, E. O. Stejskal and R. A. McKay, *J. Magn. Reson.*, 1982, **49**, 341.
35 S. R. Hartmann and E. L. Hahn, *Phys. Rev.*, 1962, **128**, 1962.
36 K. Sonogashira, Y. Tohda and N. Hagihara, *Tetrahedron Lett.*, 1975, 4467.
37 W. B. Austin, N. Bilow, W. J. Kellegham and K. S. Y. Lau, *J. Org. Chem.*, 1981, **46**, 2280.
38 P. S. Clezy and A. Liepa, *Aust. J. Chem.*, 1970, **23**, 2443.
39 DENZO: a program for film processing; Z. Otwinowski, Yale University, New Haven, 1995.
40 SCALEIT: a program for data merging and reduction; Z. Otwinowski, Yale University, New Haven, 1995.
41 SHELXL-93, G. M. Sheldrick, University of Göttingen, Göttingen, Germany, 1993.

Paper 7/04492E
Received 25*th June* 1997
Accepted 12*th December* 1997